

## Dilauroyl Peroxide의 PP에 대한 기계적, 열적 성질 변화

Kamil Şirin<sup>†</sup>, Mesut Yavuz, and Murat Çanlı

Celal Bayar University, Faculty of Science and Arts, Department of Chemistry  
(2014년 3월 11일 접수, 2014년 8월 5일 수정, 2014년 8월 6일 채택)

### Influence of Dilauroyl Peroxide on Mechanical and Thermal Properties of Different Polypropylene Matrices

Kamil Şirin<sup>†</sup>, Mesut Yavuz, and Murat Çanlı

*Celal Bayar University, Faculty of Science and Arts, Department of Chemistry, 45100, Manisa, Turkey*  
(Received March 11, 2014; Revised August 5, 2014; Accepted August 6, 2014)

**Abstract:** In this study, the influence of dilauroyl peroxide on mechanical and thermal properties of different polypropylene (PP) matrices was investigated. Polypropylene matrices, different molecular weight isotactic PP containing 0.01, 0.02, 0.04, 0.06, 0.08, and 0.1 wt% of dilauroyl peroxide (DLP) were prepared by using a single-screw extruder. The effect of the visbreaking agent (DLP) on mechanical, physical, thermal and morphological properties of different molecular weight PP had been studied. Mechanical properties (tensile strength at break point, at yield and elongation at break point), melt flow index (MFI), scanning electron microscope (SEM) and differential scanning calorimetric (DSC) analyses of these matrices were examined. Melting ( $T_m$ ) and crystallization ( $T_c$ ) temperatures, crystallinity ratio (%) and enthalpies were determined. The microstructure of isotactic polypropylene matrix was investigated by scanning electron microscopy (SEM). From SEM analysis, it was observed that the surface disorder increased by the increasing amount of DLP. As a result of DSC analyses, the crystallinity ratio of the PP matrices has varied between 1.64-7.27%. Mechanical properties of the matrices have been improved. Particularly, the mechanical tests of PP have given interesting results when compounded with 0.06-0.08 wt% dilauroyl peroxide (DLP). Mechanical properties and thermal decomposition processes were all changed by increasing the amount of DLP in the matrix structure.

**Keywords:** polypropylene matrix, mechanical properties, thermal analysis.

## Introduction

Polypropylene (PP) is a widely used versatile commodity polymer with a number of desirable properties. PP resins are being produced for a very wide range of end-use applications.<sup>1-7</sup> For that purpose, the mechanical properties of these resins have to be tailor-made to fit the performance requirements of each application. In addition to polymerization methods, PP resins having controlled molecular characteristics and therefore controlled rheological properties can be produced through well-known visbreaking operations. These operations involve the use of free radical initiators to induce chain scission reactions.<sup>8-10</sup>

The properties of polyolefin are routinely modified by

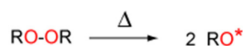
molecular structural changes caused by attack of free radicals. Free radicals formed on the main chain atoms set off a variety of reactions that end at modifying the molecular macrostructure. The free radicals can be provided by oxygen at sufficiently high temperature, peroxides decomposition, or high energy radiation.<sup>11</sup>

In recent years, controlled degradation of PP in the presence of organic peroxide-known as “vis-breaking”- has become a widely-used in industrial technology. For the peroxide-initiated degradation of PP, several models have been developed and the accepted peroxide-initiated degradation mechanism is shown in Scheme 1. The controlled degradation of PP to form a product of lower molecular weight and narrower molecular-weight distribution is commonly referred to as the product is called controlled-rheology polypropylene (CRPP).<sup>12,13</sup> The advantages of CRPP are less elasticity, less shear sensitivity, less part war page and better physical properties such as clarity

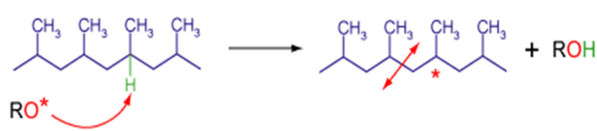
<sup>†</sup>To whom correspondence should be addressed.

E-mail: sirin.kamil@gmail.com

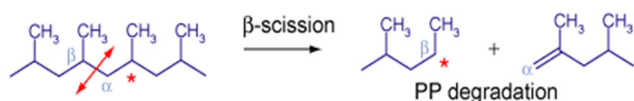
©2015 The Polymer Society of Korea. All rights reserved.



**Macroradical formation:** transfer of alkoxy radical to PP backbone



**Beta scission:** Macroradical rearrangement leading to chain scission



The macroradical can then be transferred to another PP chain.

**Scheme 1.** Degradation of polypropylene.

and gloss.<sup>14,15</sup>

Chain-scission occurs when a C-C bond near the macroradical tends to break down to two smaller fragments. This is typical in PP. The PP macroradicals tend to fragment to a secondary C-centered radical and a smaller unsaturated chain by so called  $\beta$ -scission (Scheme 1). Chain scission may take place at the secondary radicals as well, especially at high temperatures. The probability for PP macroradicals to combine with each other is lower.<sup>16,17</sup>

The focus of this study is to understand the changes on the influence of the visbreaking agent (DLP) on mechanical, physical, thermal and morphological properties of different molecular weight PP have been studied.

## Experimental

**Materials.** Isotactic polypropylene (PP-MH220, PP-MH418 and PP-EH241) were supplied as pellets by Petkim Petrochemical Company (Aliaga, Izmir, Turkey) having melt flow index values of 3.4, 5.2, and 27.0 g/10 min, respectively. Organic peroxide for controlled degradation of PP, dilauroyl peroxide, was purchased from Sigma Aldrich.

**Preparation of Matrices.** Isotactic polypropylene matrices with different amounts (0.01-0.1 wt%) DLP were prepared by melting with a single-screw extruder (Collin E 30P). The matrices were prepared by melting the mixed components in an extruder which was set at the extruder diameter: 30 mm, length to diameter ratio: 20, pressure: 7-20 bar, temperature scale samples from filing part to head: 190-250 °C and screw

**Table 1.** Sample Code and Matrices Ratio

Sample Code			PP (wt%)	DLP (wt%)
PPMH220	PPEH241	PPMH418		
aPP1	bPP1	cPP1	100	0.00
aPP2	bPP2	cPP2	99.99	0.01
aPP3	bPP3	cPP3	99.98	0.02
aPP4	bPP4	cPP4	99.96	0.04
aPP5	bPP5	cPP5	99.94	0.06
aPP6	bPP6	cPP6	99.92	0.08
aPP7	bPP7	cPP7	99.90	0.10

operation speed: 40 rev.min<sup>-1</sup>. All compounds were produced as 70  $\mu\text{m}$  thick and 10 cm wide films. Matrices ratios were prepared and their codes are given in Table 1. These matrices are called as PPMH220 (aPP1-aPP7), PPEH241 (bPP1-bPP7) and PPMH418 (cPP1-cPP7). All of these matrices were prepared as samples weighing 1000 g.

**Melt Flow Index (MFI) Measurements.** Melt flow index or melt flow rate measurements of the PP matrixes were carried out on a MFI (MP-E) Microprocessor apparatus (Tinius-Olsen, Horsham, PA, USA) at 230 °C and under a 2.16 kg weight. After a steady flow state was reached, five samples were cut sequentially and their average weight value was obtained. Experiments were done according to ASTM D-1238.

**Mechanical Testing Measurements.** Tensile testing of the samples were performed at 25 $\pm$ 1 °C at a crosshead speed of 50 mm/min according to ASTM D638, an Instron tensile tester (model 1114) was used.

Sample plates were prepared according to ASTM D-1238 and delayed 48-72 h at the laboratory conditions. These sample plates were heat-molded into sheets, which were then cut into pieces, and put into a 200 $\times$ 200 $\times$ 1 mm mold and the samples were squeezed between plates in a heating press at 230 °C under: 0 MPa for 2 min; 5 MPa for 2 min; 10 MPa for 2 min; 15 MPa for 1 min; 60 MPa for 3 min.

Afterwards, the samples were cooled to room temperature. Mould was put in a hydraulic press under pressure of 150 MPa for 3 min. Sample strips for the tests were cut from the plate ASTM 638.

Five measurements were recorded for each sample and the average values were calculated and reported. Narrow-waist dumbbell was used for tensile test specimen (ISO/DIS 527 Type A). The averages of all values were calculated for the tensile strength at yield point and break points, elongation at break point, for every one recorded.

**Differential Scanning Calorimetric Measurements (DSC).** Differential scanning calorimetric (DSC) analyses were carried out in a Shimadzu DSC-50 (Shimadzu, Kyoto, Japan) thermal analyzer in nitrogen atmosphere. The samples were heated from 25 to 200 °C at 10 °C min<sup>-1</sup>, cooled to 25 °C at the same rate, and re-heated and cooled under the same conditions. Melting ( $T_m$ ) and crystallization ( $T_c$ ) temperatures and enthalpies were determined from the second scan.  $T_m$  was considered to be the maximum of the endothermic melting peak from the heating scans and  $T_c$  that of the exothermic peak of the crystallization from the cooling scans. The heat of fusion ( $\Delta H_f$ ) and crystallization enthalpy ( $\Delta H_c$ ) were determined from the areas of melting peaks and crystallization peaks.

$$(X_c) = \frac{\Delta H_f}{\Delta H_c} \times 100$$

$\Delta H_f$  = Heat of fusion (Jg<sup>-1</sup>)

$\Delta H_c$  = 100% crystal polymer crystallization energy (Jg<sup>-1</sup>)

( $X_c$ ) = Crystallinity (%)

The various melting and crystallization parameters which were determined by means of heating and cooling scans for PP are given in Table 2.

Polymers are semicrystalline, which means that they are composed of amorphous and crystalline phases. The crystallinity is indication of amount of crystalline region in polymer with respect to amorphous content.<sup>18</sup>

The crystallinity of PP samples was calculated with the total enthalpy method; in all calculations, the heats of fusion at equilibrium melting temperature were 209 J/g for PP crystals.<sup>19</sup>

**Scanning Electron Microscopy (SEM).** Scanning electron microscopy (SEM) was used to examine the morphology of samples by using a Philips XL-305 FEG e SEM (Amsterdam, Netherland).

**Thermogravimetric Analysis (TG).** Thermogravimetric analysis (TG) curves were performed on a Seteram Labsys TG-16 (Seteram, Caluire, France) thermobalance, operating in dynamic mode, using sealed platinum pan under following conditions; sample weight ~5 mg, heating rate = 10 °C min<sup>-1</sup>, nitrogen atmosphere (10 cm<sup>3</sup> min<sup>-1</sup>).

## Results and Discussion

**Mechanical, Thermal and Morphological Properties.** The mechanical properties of PP depend on several factors and are strongly influenced by the molecular weight. General obser-

vations suggest that an increase in molecular weight, keeping all other structural parameters similar, leads to reduction in tensile strength, stiffness, hardness, brittle point but an increase in impact strength. This effect of molecular weight on the properties of PP is contrary to most other well-known plastics.<sup>20</sup>

In the study, MFI values of PP increase with the amount of DLP accordingly because of degradation (initiate  $\beta$ -scission of the PP chain) effect of peroxide on PP.

MFI values were seemed to increase for all cPP matrices. This result shows that the polymer has gone under degradation. For PP matrices, increasing DLP content has resulted serious changes on tensile strength at yield point and tensile strength at break point values. Especially for cPP4, cPP5, and cPP6 matrices these values were found to be very high. Elongation at break point values of the matrices has increased for aPP and bPP while it showed a decrease for cPP.

According to Munteanu,<sup>21</sup> a post-reactor process may also be used successfully to increase MFI of the polymer and narrow the molecular weight distribution (MWD).

The melt flow rates of PP samples increase with increasing DLP content. This is a proof of the degradation in PP samples, as shown in Figure 1.

Several vital changes were observed in tensile strength at yield point, tensile strength at break point and elongation at break point values of PP samples due to DLP content. Generally, all of these mechanical properties were improved by DLP addition. According to Figure 1, melt flow index values showed an increase depending on the amount of peroxide in PP matrices. The highest change was happened in cPP samples.

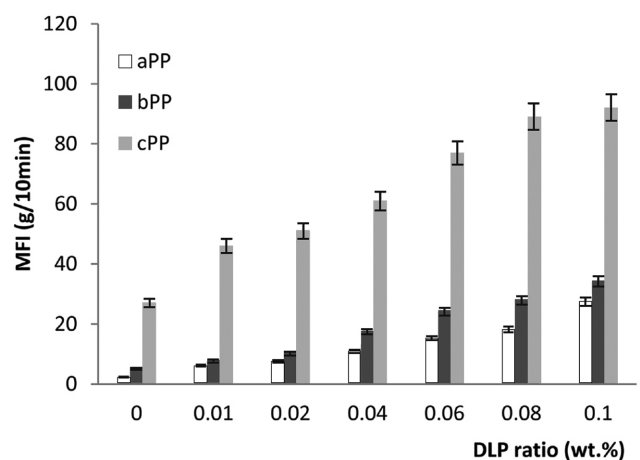


**Figure 1.** Melt flow index values of PP matrices.

In Figure 2, for PP matrices, tensile strengths at break point values show that the highest numbers seemed to be recorded in cPP samples, for considering pure PP with the highest numbers clearly observed in cPP4. cPP4 matrix seems to have very good mechanical properties with respect to cPP1.

In Figure 3, when tensile strength at yield point values of PP matrices was examined, it was seen that there is an increase following a decrease for peroxide amount of 0 to 0.04 wt%. Especially, the increase in aPP4, bPP4, and cPP4 samples was higher than other PP matrices. As seen in Figure 4, elongation at break point values of aPP samples showed an increase and then a decrease between 0 to 0.04 wt%. bPP samples showed similar values. For cPP samples, the change was nearly no change in values. Even though all the samples are PP as in main structure, each sample has a different MFI value. On page 2, cPP samples have much higher MFI values than aPP and bPP samples. All PP samples are polymers, but according to their MFI values, cPP has higher flow rate. The change in

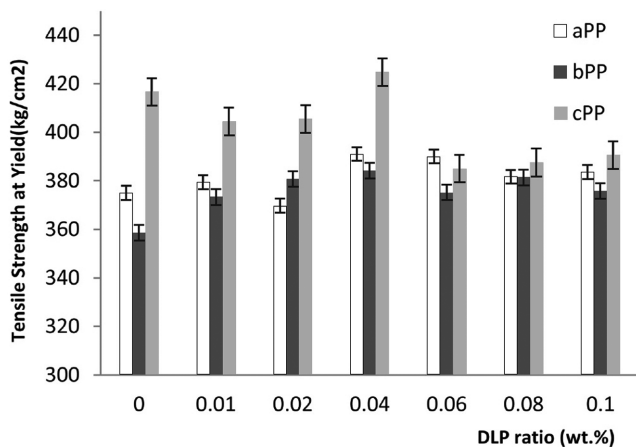


Figure 2. Tensile strength at yield point values of PP matrices.

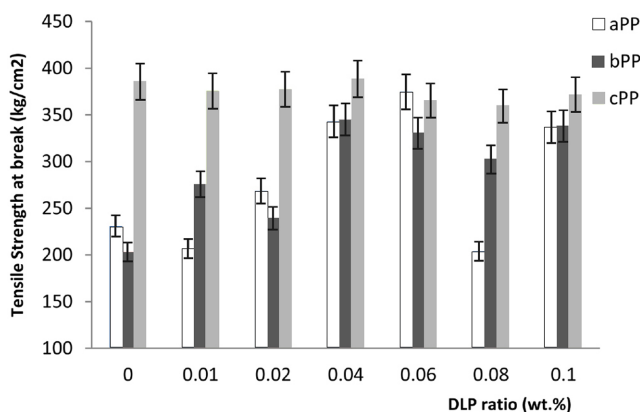


Figure 3. Tensile strength at break point values of PP matrices.

elongation at break point values for cPP seems low because it might be occurring cPP not able to catch enough DLP to create a difference.

The positive effect of DLP on tensile strength of the PP is understood as a result of the influence of its high molecular weight PP on the increase of tensile strength at yield point, tensile strength at break point values and polymer chain orientation in PP matrices. This explanation confirms the fact that practically in all cases the PP matrices prepared with DLP proved to have a higher tensile strength than ones with the absence of DLP in Figure 2 to 4.

PP is a semi-crystalline polymer. Its main, stable crystal form is the  $\alpha$  (monoclinic) form. The orientation of crystallites under stress or in the presence of some filler with a high aspect ratio, such as magnesium hydroxide or talc, can occur. It is believed that the orientation of crystallites can improve the mechanical properties. PP consists predominantly of orientations in the 110, 040, 130, 111, and 041 directions. The 110 and 040 planes are the most important and reveal information about the directions in which the  $a$  and  $b$  axes are oriented. The relationship between the orientation of PP in the  $a$  and  $b$  axes can be obtained from the ratio of the diffraction intensity of the 110 plane to that of the 040 plane. If the ratio is less than 1.3, the  $b$  axis lies predominantly to the surface under analysis. If the ratio is greater than 1.5, then the  $a$  axis is parallel to the surface.<sup>22-25</sup>

The results derived from DSC data and  $I(110)/I(040)$  values of the matrices are given on following Table 2. Endothermic melting point peaks in heating curves and crystallization peaks in cooling curves were clearly observed in Figure 5 to 7. Crystallization temperatures of aPP, cPP, and bPP samples are very close to each other and vary between 110.63 to 113.96 °C.

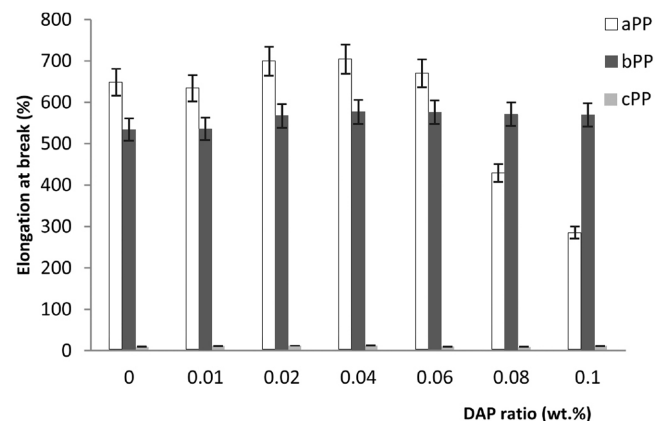
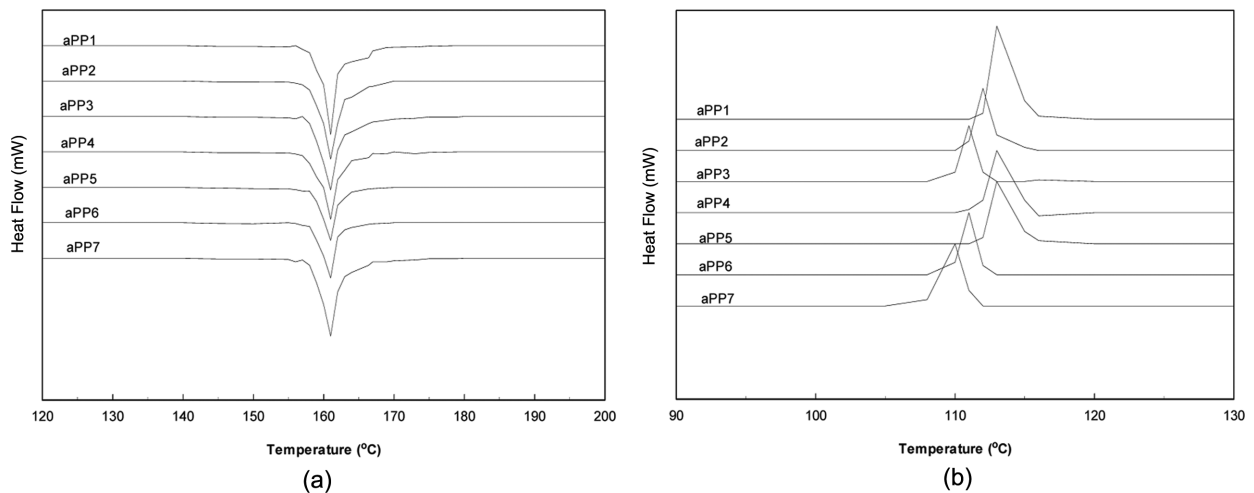


Figure 4. Elongation at break point values of PP matrices.

**Table 2. DSC Data of PP Samples**

Sample code	Melting (from second heating scans)		Crystallization (from second heating scans)			I(110)/I(040)
	$T_m$ (°C)	$\Delta H_f$ (J/g)	$T_c$ (°C)	$\Delta H_c$ (J/g)	$X_c$ (%)	
aPP1	161.97	78.45	113.49	96.41	37.54	1.81
aPP2	161.28	81.09	112.66	94.79	38.80	1.80
aPP3	160.96	80.19	111.63	90.64	38.37	1.93
aPP4	160.98	87.13	112.97	98.37	41.69	2.01
aPP5	160.74	81.45	112.32	97.60	38.97	1.95
aPP6	160.47	78.54	111.98	94.90	37.58	1.79
aPP7	160.21	77.14	110.13	96.45	36.91	1.77
bPP1	161.16	77.79	112.42	98.39	37.22	1.57
bPP2	161.11	77.67	113.92	100.81	37.16	1.59
bPP3	161.01	77.70	113.71	98.211	37.18	1.75
bPP4	160.84	84.22	113.74	101.29	40.30	1.79
bPP5	160.83	77.16	113.72	100.45	36.92	1.63
bPP6	160.85	79.56	113.77	95.752	38.07	1.77
bPP7	160.68	78.14	113.91	100.49	37.39	1.46
cPP1	162.16	80.40	113.96	92.86	38.47	1.86
cPP2	161.66	75.59	112.62	95.95	36.17	1.87
cPP3	161.33	83.72	112.25	98.34	40.06	1.88
cPP4	160.79	90.30	112.80	100.93	43.21	1.91
cPP5	160.99	89.21	112.59	96.38	42.68	1.88
cPP6	161.16	86.21	112.74	98.30	41.25	1.87
cPP7	160.79	88.42	112.64	92.13	42.31	1.86

**Figure 5.** DSC melting (a); crystallization (b) curves of aPP.

Melting points of the matrices are also close and changes between 160 to 162 °C. There is not much change in melting and crystallization temperatures by DLP addition and they are similar to the results gathered in our previous study.<sup>26</sup> The

melting and crystallization energies of PP4 matrices are dominant when compared to other matrices for all three PP types. The energy for melting initially increases by DLP addition but then decreases in higher ratios.

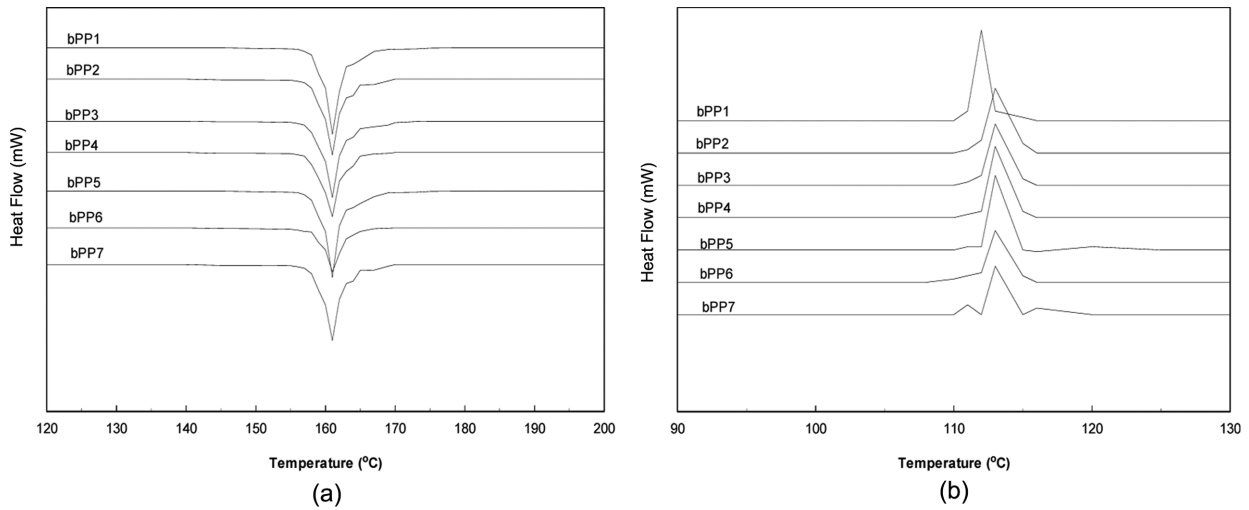


Figure 6. DSC melting (a); crystallization (b) curves of bPP.

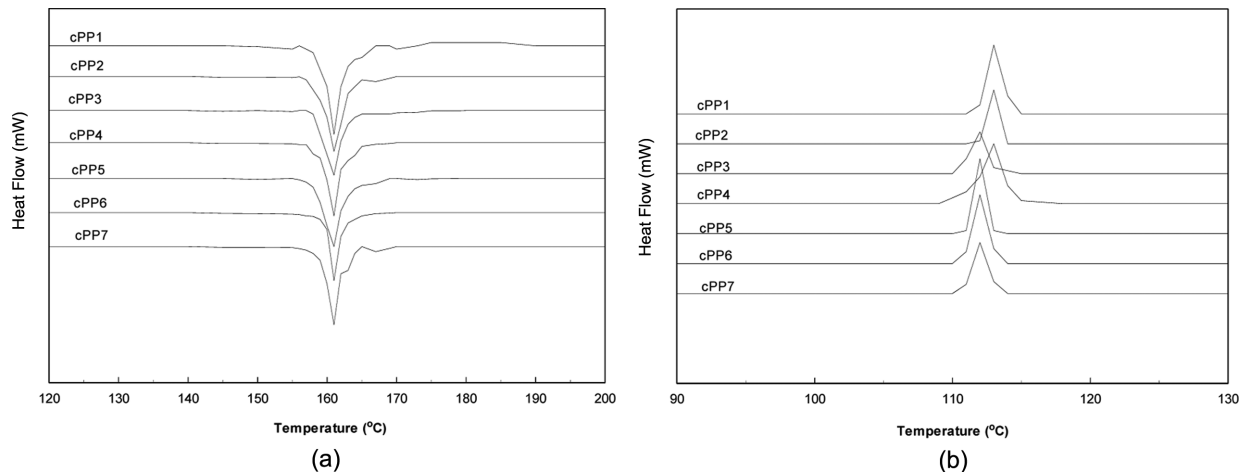


Figure 7. DSC melting (a); crystallization (b) curves of cPP.

Increasing DLP ratio has changed an increase in the crystallization ratios of all PP matrices. This ratio is approximately 7.27% in aPP matrices, 1.64% in bPP matrices and 4.74% in cPP matrices. Another considerable issue is that the crystallization ratio initially increases by DLP then decreases by further addition. The samples cPP4, cPP5, cPP7, aPP4, cPP6, and bPP4 have the highest results for thermal analyses.

X-Ray graphs of matrices are given in Figure 8 to 10. X-Ray analyses were carried out to investigate the possible crystallinity changes and orientations in PP matrices due to DLP addition. The diffraction peaks displayed in the following X-ray graphs of aPP4&aPP1 and cPP4&cPP1 matrices change between  $10^\circ$  and  $30^\circ$  which indicate cPP crystal's typical  $\alpha$  and  $\beta$  form. The peaks at  $2\theta=13.99$ ,  $16.76$ ,  $18.38$ , and  $21.71$  show the  $\alpha$ -form of the cPP matrices and the peaks at  $2\theta=16.02$  and

$21.18$  show the  $\beta$ -form. Important differences were observed in the diffraction patterns of cPP matrix crystals due to DLP addition. The intensity of the peaks belonging to  $\beta$  form at  $2\theta=16.02$  and  $21.18$  for cPP and at  $2\theta=15.98$  and  $21.02$  for aPP increases due to DLP addition. This suggests that DLP causes the structure to convert from  $\alpha$  form to  $\beta$  form. The heights of the peaks initially rise due to DLP, and then decrease. As a consequence, the crystallinity ratio (the density and the height of the peaks) in both PP types differs according to DLP ratio. This fact suits well with DSC results. The crystallinity ratios of the  $\beta$  forms in both PP types were measured by K-value proposed by Turner-Jones *et al.*<sup>27</sup>

$$K = H_{\beta 1} / (H_{\beta 1} + H_{\alpha 1} + H_{\alpha 2} + H_{\alpha 3})$$

In this equation  $H_{\alpha 1}$ ,  $H_{\alpha 2}$ , and  $H_{\alpha 3}$  are the heights of the

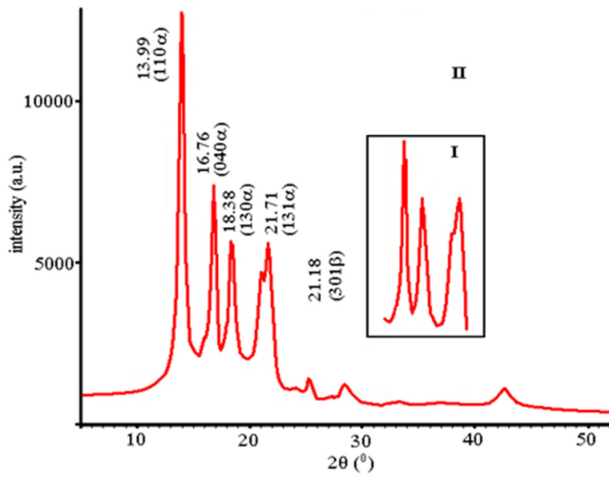


**Figure 8.** X-Ray graphs of aPP4 and aPP1 matrices (I: aPP1 matrix; II: aPP4 matrix).

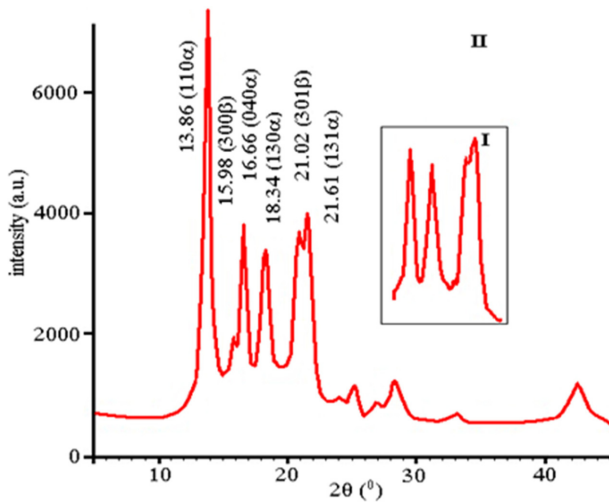


**Figure 9.** X-Ray graphs of bPP4 and bPP1 matrices (I: bPP1; II: bPP4 matrix).

peaks at  $2\theta = 13.99$ ,  $16.76$  and  $18.38$  showing (110), (040), and (130)  $\alpha$  forms of the cPP matrices, respectively.  $H_{\beta 1}$  is the height of the peak at  $2\theta = 16.02$  indicating (300)  $\beta$  crystalline form.

X-Ray graphs of aPP and cPP matrices clearly show that the intensity of (040) planes generally decreases by DLP addition whereas the intensity of (110) planes get higher as shown in Table 2. The ratio between (040) and (110) can give important clues about the orientation relation of the  $a$  and  $b$ -axes. The increase in DLP content changed the  $I(110)/I(040)$  ratio and caused the orientation through  $a$ -axis to increase. This suggests that the increasing crystallinity is through the  $a$ -axis. Excess DLP addition however decreased this type of crystallinity,

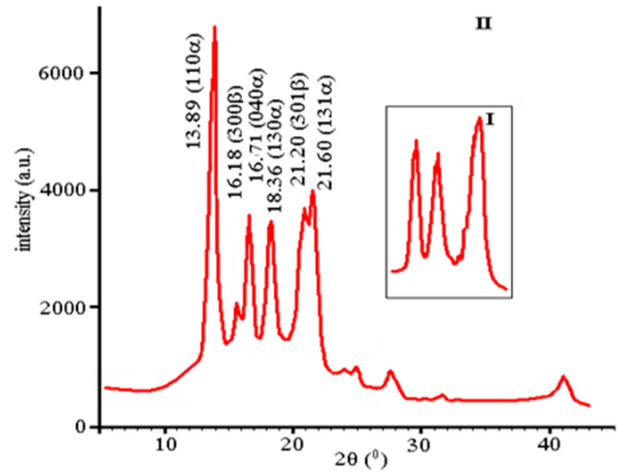


**Figure 10.** X-Ray graphs of cPP4 and cPP1 matrices (I: cPP1; II: cPP4 matrix)

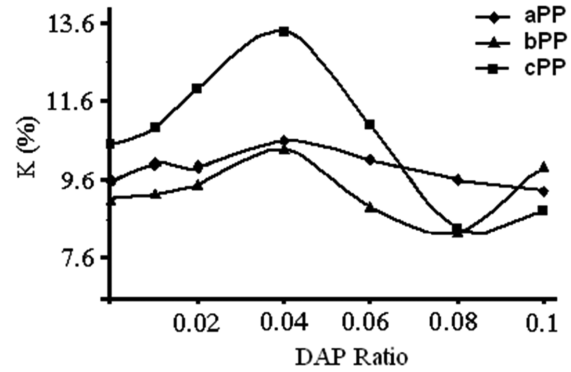


**Figure 11.** K-values of DLP treated PP matrices.

increasing orientation through  $b$ -axis.

X-Ray graphs of bPP matrix display that increasing DLP content converts bPP from  $\alpha$  form to  $\beta$  form like the other PP matrices. This conversion increases initially by DLP addition then decreases due to excess DLP content. The peaks at  $2\theta = 13.89$ ,  $16.74$ ,  $18.32$ , and  $21.74$  show the  $\alpha$ -form of the bPP matrices whereas the peaks at  $2\theta = 16.27$  and  $21.08$  show the  $\beta$ -form.

The effect of DLP on K-values is displayed in the Figure 11. As concentration of DLP gets higher, K values initially increase then decrease. The maximum K-value is observed when the ratio of DLP is 0.04 wt% K-value of PP matrices considerably changed due to increasing DLP ratio. The results demonstrate that increasing DLP content in PP matrices increases the  $\beta$ -form of the matrices when decreasing the  $\alpha$ -form. Thus, DLP can be used as a tool to increase the  $\beta$ -form of PP matrices.

In all of the PP matrices, the matrix that has 0.04 wt% DLP

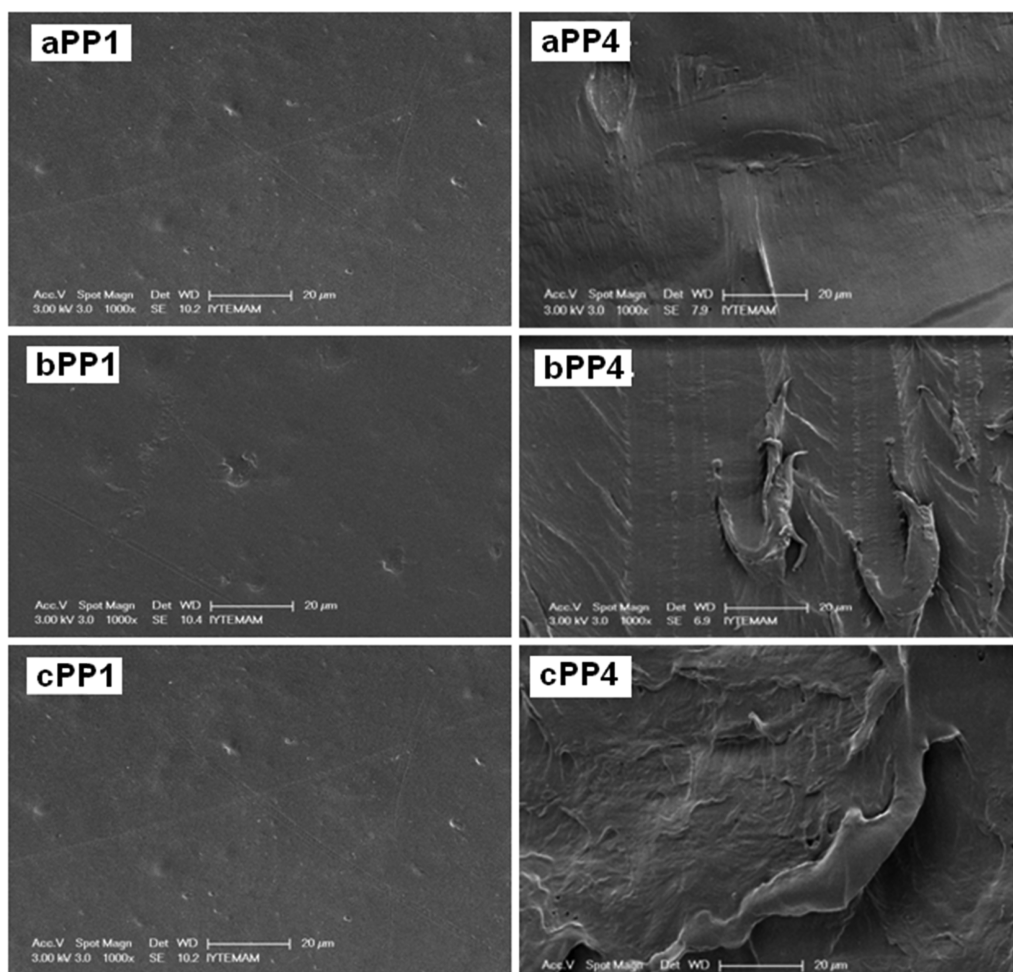


**Figure 12.** SEM images of PP1 and PP4 matrices.

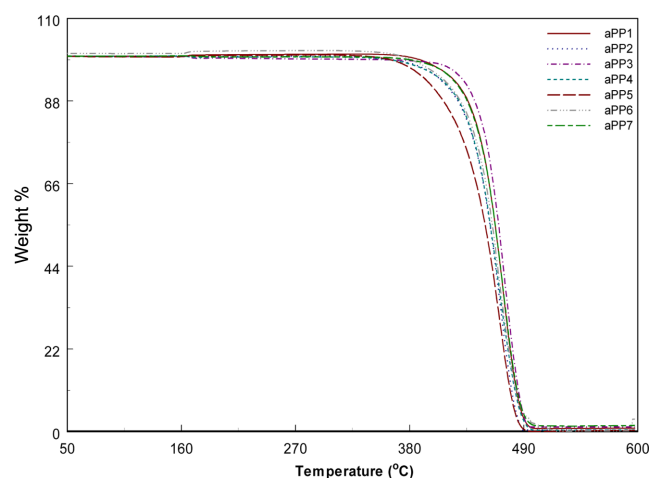
was observed to be dominant.

SEM images of the PP1 and PP4 matrices are given in Figure 12. Considerably regular channels have been spotted in the structure of PP4. These channels can be the border lines of  $\alpha$  and  $\beta$  form. At lower concentrations of DLP the channels were not formed regularly, at higher concentrations however the channels were observed to deform. These results indicate that related borders have direct effect to the mechanical properties and crystallinity ratios of PP matrices. Interesting images were obtained from the SEM micrographs of aPP matrices. According to these images, adding peroxide has caused a homogeny structure in aPP4 sample.

The other SEM pictures show that bPP4 and cPP4 samples are alike to each other. The SEM pictures point out that there is an effect of DLP for all PP samples without exception.

**Thermal Properties.** TG curves of the PP matrices obtained at a heating rate of  $10\text{ }^{\circ}\text{C}\cdot\text{min}^{-1}$  are shown in Figure 13 to 15. All the thermogravimetric curves are in similar character

and symmetric. TG curves showed that the thermal degradation of PP matrices took place in one stage. Residue weight percentage values of the samples were examined in detailed

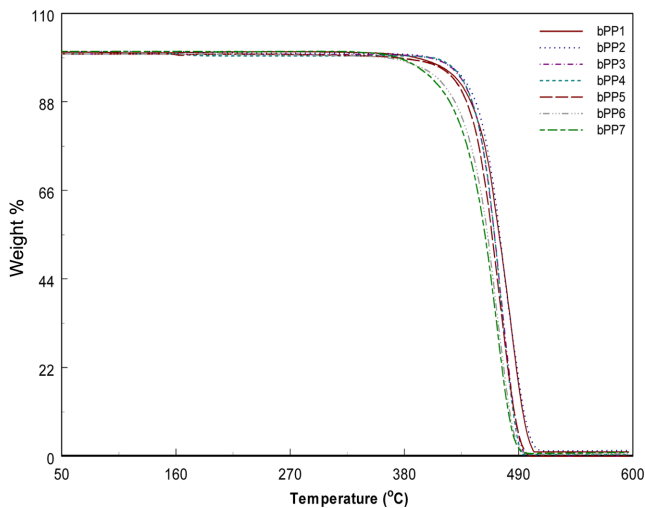


**Figure 13.** TG curves of aPP matrices.

**Table 3. Thermal Degradation Values of PP Samples**

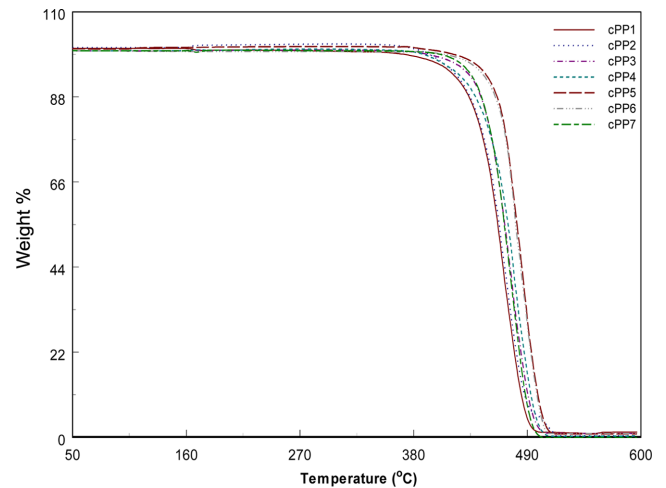
Sample code	Conversion (%)	$T_i$ (°C) <sup>a</sup>	$T_{max}$ (°C) <sup>b</sup>	$T_f$ (°C) <sup>c</sup>	Residue weight percentage			Char yield (% w <sub>t</sub> )
					400 °C	450 °C	500 °C	
aPP1	0.13-99.7	390	465	498	1.7	42.6	99.7	0.03
aPP2	0.01-99.9	364	460	488	2.0	43.2	99.9	0.01
aPP3	0.01-99.8	360	468	494	2.2	44.6	99.8	0.02
aPP4	0.01-99.9	361	461	495	2.2	42.4	99.5	0.05
aPP5	0.01-99.8	362	456	489	2.2	43.9	99.8	0.02
aPP6	0.01-99.8	382	462	496	1.5	44.0	99.8	0.02
aPP7	0.01-99.8	379	465	493	1.6	45.7	99.8	0.02
bPP1	0.01-99.6	371	464	503	1.6	42.6	98.5	0.15
bPP2	0.01-99.5	395	465	516	1.3	43.8	97.2	0.28
bPP3	0.01-99.8	394	471	537	1.2	41.6	95.4	0.46
bPP4	0.01-99.4	389	474	506	1.2	38.8	98.8	0.22
bPP5	0.01-99.7	419	482	505	0.01	43.5	98.7	0.23
bPP6	0.01-99.8	410	481	509	0.01	42.6	99.4	0.06
bPP7	0.01-99.8	406	470	501	0.5	44.8	99.8	0.02
cPP1	0.01-99.7	392	474	510	1.3	41.0	97.4	0.26
cPP2	0.01-99.4	406	474	511	0.6	42.2	96.3	0.37
cPP3	0.02-99.8	404	469	495	0.5	42.6	99.4	0.06
cPP4	0.03-99.5	406	469	492	0.5	43.1	99.6	0.04
cPP5	0.01-99.8	373	467	497	1.7	43.1	99.5	0.05
cPP6	0.01-99.6	363	463	494	1.9	40.6	99.6	0.04
cPP7	0.01-99.8	374	461	493	1.7	42.7	99.8	0.02

<sup>a</sup> $T_i$ : initiated composition temperature based upon 1% weight loss. <sup>b</sup> $T_{max}$ : decomposition temperature based upon 50% weight loss. <sup>c</sup> $T_f$ : decomposition temperature based upon 99% weight loss.

**Figure 14.** TG curves of bPP matrices.

conversion (%).

Increasing of DLP content in PP matrices leads usually to increase of all of the characteristic temperature values on the thermogravimetric curves up to a certain value. It is shown

**Figure 15.** TG curves of cPP matrices.

also that the rate curve related to matrices shift to a higher temperature. Further increase of DLP content caused stability and all characteristic values to decline due to structural deformations. PP matrix was found to have the minimum stability.

PP3 is more stable than other matrices due to its crystallinity rate. Also, two exothermic thermal effects at different temperature in DSC profiles correspond to the crystallization and decomposition of matrices.

## Conclusions

Isotactic polypropylene matrices with different amounts (0.01 to 0.1 wt%) DLP were prepared by melting with a single-screw extruder.

In our study, organic peroxide was used for controlled degradation of PP's and significant changes in the mechanical and thermal properties were observed despite the use of very small amounts DLP (0.01 to 0.1 wt%). Between 0.01 to 0.1 wt% of DLP it has a positive effect on the PP samples, but over 0.1 wt% of DLP the mechanical values start to decrease.<sup>26</sup>

- The best DLP ratio was between 0.04 wt% and it was changed inverse proportionally with MA of PP. The major change is observed in samples of bPP.
- MFI values of all PP matrices have been increased by DLP addition indicating that the polymer matrices have gone under degradation.
- Thermal analyses results had the best values. Adding DLP to PP had caused similar results for both thermal analyses and mechanical properties.
- As concentration of DLP gets higher, K values initially increase then decrease. The maximum K value is observed when the ratio of DLP is 0.04 wt%, K value of PP matrices considerably changed due to increasing DLP ratio.

The addition of very small amount of DLP to PP can be effectively used in many areas of industry.

**Acknowledgment.** This study supported by the research funds of Celal Bayar University (Project No: FEF-2012-111). Authors are thanks to Petkim Petrochemical Company (Aliaga, Izmir, Turkey) for preparation of all PP matrices.

## References

1. F. H. Su and H. X. Huang, *Adv. Polym. Technol.*, **28**, 16 (2009).
2. P. R. S. Leite, S. B. Goares, and A. S. Siqueira, *J. Appl. Polym. Sci.*, **120**, 981 (2011).
3. Y. Xu, C. Chen, L. Cao, and X. Cao, *Mater. Chem. Phys.*, **138**, 63 (2013).
4. S. H. Ahn and D. S. Kim, *Polymer(Korea)*, **38**, 129 (2014).
5. X. Chena and C. Jiaoa, *Polym. Adv. Technol.*, **22**, 817 (2011).
6. T. N. Iana, X. Wena, J. Gongga, L. Maa, J. Xuea, and T. Tanga, *Polym. Adv. Technol.*, **24**, 653 (2013).
7. K. Choi, H. S. Lee, B. C. Kang, and H. Yang, *Polymer(Korea)*, **34**, 294 (2010).
8. H. Azizi and I. Ghasemi, *Polym. Test.*, **23**, 137 (2004).
9. B. Kalantari, R. S. Rahbar, M. R. M. Mojtahedi, S. A. M. Shoushtari, and A. Khosroshahi, *J. Appl. Polym. Sci.*, **105**, 2287 (2007).
10. E. S. G. Cheverrigaray, R. C. D. Cruz, and R. V. B. Oliveira, *Polym. Bull.*, **70**, 1237 (2013).
11. C. J. Pérez, M. D. Failla, and J. M. Carella, *Polym. Degrad. Stab.*, **98**, 177 (2013).
12. H. Azizi, I. Ghasemi, and M. Karrabi, *Polym. Test.*, **27**, 548 (2008).
13. M. Aubert, M. Roth, R. Pfaendner, and C. E. Wilen, *Macromol. Mater. Eng.*, **292**, 707 (2007).
14. P. D. Iedema, K. Remerie, M. vanderHam, E. Biemond, and J. Tacx, *Chem. Eng. Sci.*, **66**, 5474 (2011).
15. Y. W. Seo and D. S. Kim, *Polymer(Korea)*, **38**, 327 (2014).
16. K. Şirin and M. Balcan, *Polym. Adv. Tech.*, **21**, 250 (2010).
17. H. G. Karain, *Handbook of Polypropylene and Polypropylene Composites*, Second Edition, Marcel Dekker, Inc., New York, 2003.
18. R. O. Ebewele, *Polymer Science and Technology*, CRC Press, Boca Raton, FL, 2000.
19. J. Brandrup, E. H. Immergut, E. A. Grulke, A. Abe, and D. R. Bloch, *Polymer Handbook*, Fourth Edition, John Wiley and Sons, New York, 2005.
20. D. Tripathi, *Practical Guide to Polypropylene*, Rapra Technology, Ltd., p 32 (2002).
21. D. Munteanu, *Plastic Additives Handbook*, Hanser, Munich-Cincinnati, 2001.
22. M. Cook and J. F. Harper, *Polym. Adv. Technol.*, **17**, 53 (1998).
23. M. Fujiyama and T. Wakino, *J. Appl. Polym. Sci.*, **42**, 2739 (1991).
24. F. Rybnikar, *J. Appl. Polym. Sci.*, **38**, 1479 (1989).
25. H. Xia, Q. Wang, K. Li, and G. H. Hu, *J. Appl. Polym. Sci.*, **93**, 378 (2004).
26. K. Şirin, F. Doğan, M. Çanlı, and M. Yavuz, *Polym. Adv. Technol.*, **24**, 715 (2013).
27. A. Turner-Jones, J. M. Aizlewood, and D. R. Beckett, *Makromol. Chem.*, **75**, 134 (1964).